

## First observation of the charmless decay of $\Xi_b^- \rightarrow pK^-K^-$ at LHCb

A. MATHAD<sup>(\*)</sup>

*Department of Physics, University of Warwick - Coventry, UK*

received 16 September 2017

**Summary.** — We present here the search for  $\Xi_b^-$  and  $\Omega_b^-$  baryon decays to the charmless hadronic final states  $ph^-h'^-$  at the LHCb detector, where  $h^{(\prime)}$  denotes a kaon or pion. The analysis is based on a sample of proton-proton collision data collected at centre-of-mass energies  $\sqrt{s} = 7$  and 8 TeV, corresponding to an integrated luminosity of  $3 \text{ fb}^{-1}$ . We observe the decay of  $\Xi_b^- \rightarrow pK^-K^-$  with a significance of 8.7 standard deviations, and evidence at the level of 3.4 standard deviations is found for the  $\Xi_b^- \rightarrow pK^-\pi^-$  decay. This result is the first ever observation of a  $\Xi_b^-$  baryon decaying into charmless final state.

### 1. – Motivation

The production of  $b$  baryons in unprecedented quantities at LHCb has opened up a new field in flavour physics for precision measurement. Of particular interest are the decays of heavy  $b$  baryons to suppressed charmless final states. Such decays proceed through tree ( $b \rightarrow u$  transition) and loop-level ( $b \rightarrow d$  or  $b \rightarrow s$  transitions) amplitudes, which, when they have similar magnitude, can interfere to give rise to large Charge-Parity ( $CP$ ) asymmetries and thus could allow a first observation of  $CP$  violation in the baryon sector. The phenomenon of  $CP$  violation is accommodated in the Standard Model (SM) through a single irreducible complex phase in the Cabibbo-Kobayashi-Maskawa (CKM) matrix [1, 2]. It is however not sufficient to address the baryon asymmetry problem and hence it is of interest to search for additional sources of  $CP$  violation. Since the amplitudes through which these decays proceed are also sensitive to contributions from physics beyond the SM, these decays act as a fertile ground for testing the SM and constraining New Physics effects.

The  $b$ -meson sector has been extensively explored by the  $B$  factories and at hadron colliders. Large  $CP$ -violation effects were observed in  $\bar{B}^0 \rightarrow K^-\pi^+$  [3-5] and  $\bar{B}_s^0 \rightarrow K^+\pi^-$  [5] decays<sup>(1)</sup>. Even larger effects have been observed in regions of the phase

<sup>(\*)</sup> On behalf of the LHCb Collaboration.

<sup>(1)</sup> The inclusion of charge-conjugate processes is implied throughout.

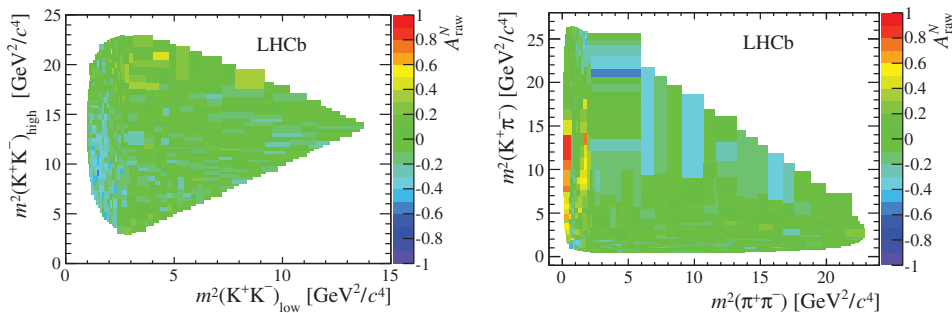


Fig. 1. – Raw asymmetry ( $A_{raw}^N$ ) as a function of Dalitz plot variables is shown for (left)  $B^- \rightarrow K^+ K^- K^-$  and (right)  $B^- \rightarrow \pi^+ K^- \pi^-$  decays. Large negative and positive asymmetries are visible at low values of  $m^2(K^- K^+)_{low}$  and  $m^2(\pi^- \pi^+)$  for  $B^- \rightarrow K^+ K^- K^-$  and  $B^- \rightarrow \pi^+ K^- \pi^-$  decays, respectively [8].

space for the decays of  $B^-$  to  $\pi^+ \pi^- \pi^-$ ,  $\pi^+ K^- \pi^-$ ,  $K^+ K^- K^-$  and  $K^+ K^- \pi^-$  final states [6-8].

As an example, we show the variation of raw asymmetries ( $A_{raw}^N = \frac{N^- - N^+}{N^- + N^+}$  where  $N^-$  and  $N^+$  corresponds to number of  $B^-$  and  $B^+$  decays respectively) as a function of Dalitz plot variables [9] for  $B^- \rightarrow K^+ K^- K^-$  and  $B^- \rightarrow \pi^+ K^- \pi^-$  in fig. 1.

In the  $b$  baryon sector, the decays of  $A_b^0$  baryon to  $p\pi^-$ ,  $pK^-$  [10],  $K_s^0 p\pi^-$  [11],  $\Lambda\phi$  [12],  $\Lambda K^+ K^-$  and  $\Lambda K^+ \pi^-$  [13] final states have been investigated. The  $CP$ -violation parameters measured in these decays are all consistent with  $CP$  symmetry. Recently, however, the first evidence of  $CP$  violation in the  $b$  baryon sector has been reported from an analysis of  $\Lambda_b^0 \rightarrow p\pi^- \pi^+ \pi^-$  decays [14]. These decays of  $\Lambda_b^0$  baryons are the only charmless hadronic  $b$  baryon decays that had been observed until now.

Here we report on the search for strange-beauty baryon (such as  $\Xi_b^- (sbd)$  or  $\Omega_b^- (ssb)$ ) decays to  $ph^- h'^-$ , where  $h^{(\prime)}$  denotes a kaon or pion. No theoretical results on branching fractions for  $\Xi_b^- (\Omega_b^-) \rightarrow ph^- h'^-$  existed prior to this analysis. Recently, however, there have been theoretical predictions for the absolute branching fractions for the  $\Xi_b^- \rightarrow R(\rightarrow ph^-)h'^-$  where  $R$  is an intermediate resonance state such as  $N, \Lambda, \Xi, \Sigma$  [15]. It would be very interesting to test these predictions and investigate  $CP$  violation effects through an amplitude analysis when a larger data sample becomes available.

Since this report summarises the published paper in ref. [16], the readers are encouraged to refer to the paper for more details.

## 2. – Analysis

In the SM, the decay of  $\Xi_b^- \rightarrow pK^- K^-$  is CKM suppressed at tree-level and loop-level. The tree-level diagram proceeds via  $b \rightarrow u$  transition whereas the loop-level diagram proceeds via  $b \rightarrow s$  transition as illustrated in fig. 2. For the cases of  $\Omega_b^- \rightarrow pK^- K^-$  and  $\Xi_b^- \rightarrow pK^- \pi^-$  decays, the tree-level and loop-level diagrams proceed via  $b \rightarrow u$  and  $b \rightarrow d$  transitions respectively. Diagrams for  $\Omega_b^- \rightarrow pK^- \pi^-$  and both  $\Xi_b^-$  and  $\Omega_b^- \rightarrow p\pi^- \pi^-$  require additional weak interaction vertices. The rates of these decays are therefore expected to be further suppressed. Additionally, fewer  $\Omega_b^-$  baryons are produced compared to  $\Xi_b^-$  baryons in the proton-proton collisions due to the lower fragmentation fraction of  $\Omega_b^-$ ,  $f_{\Omega_b^-}$ , compared to  $f_{\Xi_b^-}$ . The fragmentation fractions quantify the probabilities

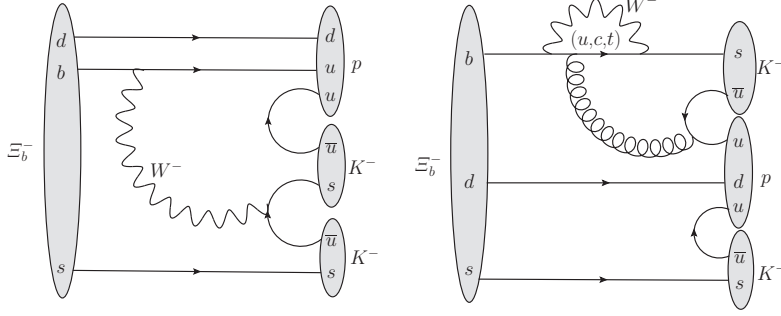


Fig. 2. – (Left) tree and (right) loop diagrams for the  $\Xi_b^- \rightarrow pK^-K^-$  decay channel.

for a  $b$  quark to hadronise into these particular states. These quantities for  $\Xi_b^-$  and  $\Omega_b^-$  baryons have not yet been determined and hence it is not possible for us to measure absolute branching fractions. Therefore, in this analysis, we measure the product of each branching fraction and the relevant fragmentation fraction relative to the corresponding values for the topologically similar normalisation channel  $B^- \rightarrow K^+K^-K^-$  (the  $B^-$  fragmentation fraction is denoted  $f_u$ ) as shown in eq. (1),

$$\begin{aligned}
 (1) \quad R_{ph-h'^-} &\equiv \frac{f_{\Xi_b^-}(\Omega_b^-) \mathcal{B}(\Xi_b^-(\Omega_b^-) \rightarrow ph^-h'^-)}{f_u \mathcal{B}(B^- \rightarrow K^+K^-K^-)} \\
 &= \frac{\mathcal{N}(\Xi_b^-(\Omega_b^-) \rightarrow ph^-h'^-) \epsilon(B^- \rightarrow K^+K^-K^-)}{\mathcal{N}(B^- \rightarrow K^+K^-K^-) \epsilon(\Xi_b^-(\Omega_b^-) \rightarrow ph^-h'^-)},
 \end{aligned}$$

where  $\epsilon$  is the efficiency of the selection and  $\mathcal{N}$  is the yield of the signal or normalisation channel after the full selection has been applied to the data sample.

The strategy employed in the signal selection to improve the purity of the data sample is summarised in sect. 2.1. The fit model to extract  $\mathcal{N}$  is summarised in sect. 2.2.

The analysis is conducted using the proton-proton collision data sample, recorded by the LHCb experiment at centre-of-mass energies  $\sqrt{s} = 7$  and 8 TeV, corresponding to  $3\text{fb}^{-1}$  of integrated luminosity.

It is important to note here that, since these decay modes have not been investigated before, we conduct a blind analysis where the candidates with invariant masses in windows around the  $\Xi_b^-$  and  $\Omega_b^-$  masses were not inspected until the selection and fit model were finalised, in order to avoid experimenter's bias entering the analysis.

**2.1. Signal selection and efficiency.** – A series of requirements have been imposed on the data sample to select signal-like candidates to improve the purity of the data sample. These requirements are summarised as follows.

**2.1.1. Online selection.** The LHCb trigger system performs online event selection [17]. It has a hardware stage, which imposes kinematic requirements on the particles in an event based on the information from the calorimeter and muon systems. It also includes a software stage which applies a full event reconstruction. Events are retained requiring the presence of tracks that are found to be consistent with originating from a  $b$ -hadron decay, on the basis of their kinematic and topological variables.

**2.1.2. Offline selection.** To further reduce the background contamination, an offline selection of  $b$ -hadron candidates formed from three tracks is carried out. It consists of the following stages.

- **Pre-filtering stage:** in this stage, further requirements on the kinematic and topological variables are imposed to retain good quality tracks originating from a vertex that is displaced from the primary  $pp$  interaction vertex (PV) and hence consistent with being a  $b$ -hadron decay. Candidates are retained if they satisfy two conditions of the hardware trigger. The positive hardware-trigger decision has to be caused either by the candidate depositing enough energy in the hadronic calorimeter, or by other particles in the event. It is also required that the software trigger decision must have been caused by the signal candidate.
- **Neural network:** to reduce contributions from candidates that are formed from random combinations of tracks in an event (combinatorial background), we train a neural network [18] formed of one hidden layer with a set of 9 kinematic and topological variables that show good separation between background and signal samples. The signal and background samples are obtained from the  $B^- \rightarrow K^+K^-K^-$  channel, using a data-driven approach in which the two components are separated statistically using the *sPlot* method [19] with the  $b$ -candidate mass as discriminating variable. It was checked that the distributions of these variables are consistent between simulated samples of signal decays and the  $B^- \rightarrow K^+K^-K^-$  normalisation channel, and between background-subtracted  $B^- \rightarrow K^+K^-K^-$  data and simulation. The requirement on the neural network output is optimised using a figure of merit [20] incorporating the estimated signal efficiency and number of background events. The signal efficiency of this requirement is about 60% with a background rejection of approximately 70%. The same neural network output requirement is made for all final states.
- **Particle identification (PID):** to minimise the background contamination from the mis-identification of one or more final state particles (cross-feed background) and to further reduce combinatorial background, we apply PID requirements on the final state tracks. Using information from the ring-imaging Cherenkov detectors, the decay products are identified uniquely as protons, kaons and pions [21]. The combined efficiency of the PID requirements is about 30% for the  $pK^-K^-$ , 40% for the  $pK^-\pi^-$  and 50% for the  $p\pi^-\pi^-$  final state. The single particle mis-identification rates associated with this requirement for mis-identifying  $\pi \rightarrow K$ ,  $K \rightarrow \pi$ ,  $\pi \rightarrow p$  and  $K \rightarrow p$  are approximately 0.8%, 9%, 0.2% and 0.2% respectively. The rates associated with double particle mis-identification for  $\pi\pi \rightarrow KK$ ,  $KK \rightarrow \pi\pi$ ,  $KK \rightarrow \pi p$ ,  $\pi\pi \rightarrow Kp$  and  $\pi K \rightarrow Kp$  are approximately 0.02%, 2%, 0.05%, 0.005% and 0.05%, respectively.
- **Charm vetoes:** to ensure that any signal seen is due to charmless decays, candidates with  $pK^-$  invariant mass consistent with the  $\Xi_b^- \rightarrow \Xi_c^0 h^- \rightarrow pK^- h^-$  or  $\Xi_b^- \rightarrow \Xi_c^0 h^- \rightarrow p\pi^- h^-$  decay chain are vetoed. Similarly, candidates for the normalisation channel with  $K^+K^-$  invariant mass consistent with the  $B^- \rightarrow D^0 (\rightarrow K^+K^-)K^-$  decay chain are removed.

The efficiencies of the signal selection (taking into account detector geometry, reconstruction, online and offline selection criteria) are determined from simulation except for

TABLE I. – Fitted yields, efficiencies and relative branching fractions multiplied by fragmentation fractions ( $R_{ph^-h'^-}$ ). The two uncertainties quoted on  $R_{ph^-h'^-}$  are statistical and systematic. Upper limits are quoted at 90 (95)% CL for modes with signal significance less than  $3\sigma$ . Uncertainties on the efficiencies are not given as only the relative uncertainties affect the branching fraction measurements.

Mode	Yield $\mathcal{N}$	Efficiency $\epsilon$ (%)	$R_{ph^-h'^-}$ ( $10^{-5}$ )
$\Xi_b^- \rightarrow pK^-K^-$	$82.9 \pm 10.4$	0.398	$265 \pm 35 \pm 47$
$\Xi_b^- \rightarrow pK^- \pi^-$	$59.6 \pm 16.0$	0.293	$259 \pm 64 \pm 49$
$\Xi_b^- \rightarrow p\pi^- \pi^-$	$33.2 \pm 17.9$	0.573	$74 \pm 40 \pm 36 < 147$ (166)
$\Omega_b^- \rightarrow pK^-K^-$	$-2.8 \pm 2.5$	0.375	$-9 \pm 9 \pm 6 < 18$ (22)
$\Omega_b^- \rightarrow pK^- \pi^-$	$-7.6 \pm 9.2$	0.418	$-23 \pm 28 \pm 23 < 51$ (62)
$\Omega_b^- \rightarrow p\pi^- \pi^-$	$20.1 \pm 13.8$	0.536	$48 \pm 33 \pm 28 < 109$ (124)
$B^- \rightarrow K^+K^-K^-$	$50\,490 \pm 250$	0.643	–

that of the PID criteria, which is determined from data control samples weighted according to the expected kinematics of the signal tracks [22]. Table I shows the total signal selection efficiency,  $\epsilon$ .

These efficiencies are determined as a function of the position in phase space in each of the three-body final states. For channels with significant signal yields, efficiency corrections for each candidate are applied to take the variation of efficiency over the phase space into account. For channels without significant signal yields the efficiency averaged over phase space is used in eq. (1).

**2.2. Signal yield extraction.** – A simultaneous unbinned extended maximum likelihood fit to the  $b$  baryon candidate mass distributions in the three  $ph^-h'^-$  final states is carried out to extract the yields of the signal decays. The yield of the normalisation channel is determined from a separate fit to the  $K^+K^-K^-$  mass distribution. The different components of the total PDF are listed as follows.

- Each signal component is modelled with the sum of two Crystal Ball (CB) functions [23] with shared parameters describing the core width and peak position and with non-Gaussian tails to both sides.
- Cross-feed backgrounds from other signal decays to  $ph^-h'^-$  final states are also modelled with the sum of two CB functions. Cross-feed backgrounds from  $B^- \rightarrow K^+h^-h'^-$  decays are modelled, in the mass interval of the fit, by exponential functions. The yields of all cross-feed backgrounds are constrained to their expected values, which is calculated using yields taken from the fit to the correctly reconstructed spectrum and the mis-identification rates.
- Partially reconstructed backgrounds arise due to  $b$ -hadron decays into final states similar to the signal, but with additional soft particles that are not reconstructed. Possible examples include  $\Xi_b^- \rightarrow N^+h^-h'^- \rightarrow p\pi^0h^-h'^-$  and  $\Xi_b^- \rightarrow pK^{*-}h^- \rightarrow pK^-\pi^0h^-$ . Such decays are investigated with simulation and it is found that many of them have similar  $b$  baryon candidate mass distributions. The shapes of these backgrounds are modelled with an ARGUS function [24] convolved with a Gaussian function and are taken from  $\Xi_b^- \rightarrow N^+h^-h'^- \rightarrow p\pi^0h^-h'^-$  simulated decay.

- The combinatorial background is modelled by an exponential function with the shape parameter shared between the three final states.

For all the above components, the shape parameters are either fixed to known values or determined from simulation. Some data-simulation differences are determined from the normalization mode fit and used in the signal shape.

The results of the fits are shown in fig. 3 and the obtained signal yields are shown in table I.

### 3. – Results

We observe the decay  $\Xi_b^- \rightarrow pK^-K^-$  with a significance of  $8.7\sigma$  and see evidence of the  $\Xi_b^- \rightarrow pK^- \pi^-$  decay at a significance of  $3.4\sigma$ . All the other decay modes have significance less than  $2\sigma$ .

The results for  $R_{ph-h'}$ , which is defined in eq. (1), are reported in table I. When the signal significance is less than  $3\sigma$ , upper limits are set at 90 (95%) Confidence Level (CL). The sources of systematic uncertainty arising from the fit model and the knowledge of the efficiency are taken into account in this analysis. For modes observed with significance  $> 3\sigma$ , the dominant source of systematic uncertainty arises due to the mis-match of  $\Xi_b^-$  production kinematics in simulation and data. For modes observed with

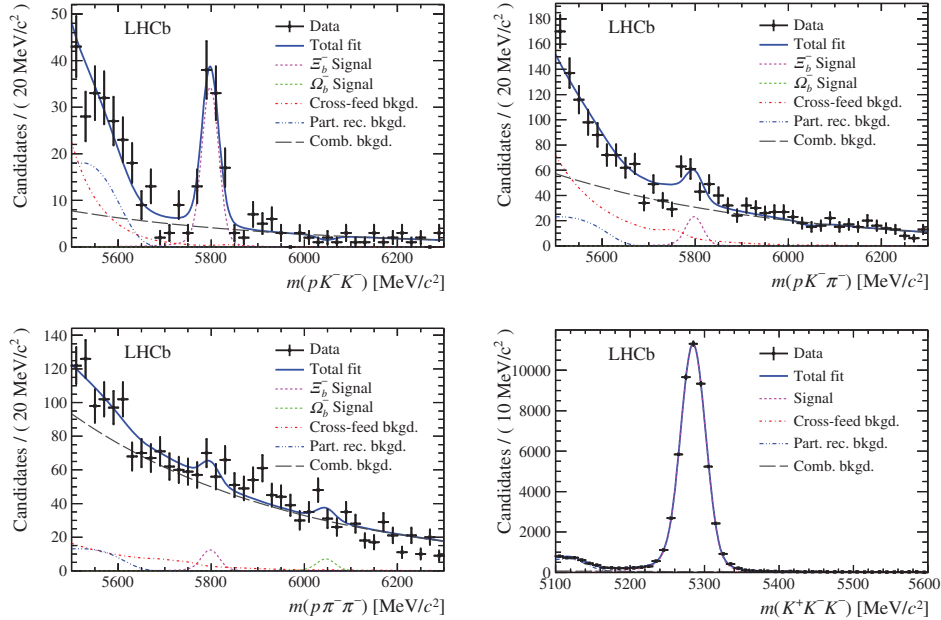


Fig. 3. – Mass distributions for  $b$ -hadron candidates in the (top left)  $pK^-K^-$ , (top right)  $pK^- \pi^-$ , (bottom left)  $p\pi^- \pi^-$  and (bottom right)  $K^+K^-K^-$  final states. Results of the fits are shown with dark blue solid lines. Signals for  $\Xi_b^-$  and  $B^-$  ( $\Omega_b^-$ ) decays are shown with pink (light green) dashed lines, combinatorial backgrounds are shown with grey long-dashed lines, cross-feed backgrounds are shown with red dot-dashed lines, and partially reconstructed backgrounds are shown with dark blue double-dot-dashed lines [16].

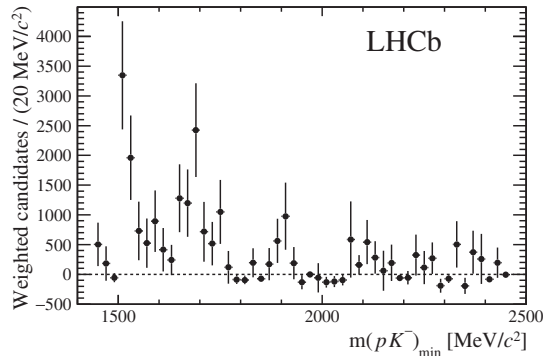


Fig. 4. – Efficiency-corrected and background-subtracted [19]  $m(pK^-)_{\min}$  distribution of  $\Xi_b^- \rightarrow pK^- K^-$  candidates [16].

significance  $< 3\sigma$ , the dominant source of systematic uncertainty arises from variation of the efficiency over the phase space.

The yield of  $\Xi_b^- \rightarrow pK^- K^-$  decays is sufficient to use as normalisation for the relative branching fractions of the other  $\Xi_b^-$  decays, which are quoted below.

$$\frac{\mathcal{B}(\Xi_b^- \rightarrow pK^- \pi^-)}{\mathcal{B}(\Xi_b^- \rightarrow pK^- K^-)} = 0.98 \pm 0.27 \text{ (stat)} \pm 0.09 \text{ (syst)},$$

$$\frac{\mathcal{B}(\Xi_b^- \rightarrow p\pi^- \pi^-)}{\mathcal{B}(\Xi_b^- \rightarrow pK^- K^-)} = 0.28 \pm 0.16 \text{ (stat)} \pm 0.13 \text{ (syst)} < 0.56 \text{ (0.63)},$$

where the upper limit is quoted at 90 (95)% CL. For these above quantities the previous sources of systematic uncertainties mostly cancel out in the ratio, the dominant source of systematic uncertainties here being the residual differences in the trigger efficiency between data and simulation, the fit model and, for the  $\Xi_b^- \rightarrow p\pi^- \pi^-$  mode, the efficiency variation across the phase space.

Since the signal modes we are investigating are all three-body decays, they will have contributions from quasi-two body decays. Therefore, we also show here the efficiency-corrected and background-subtracted  $m(pK^-)_{\min}$  distribution for  $\Xi_b^- \rightarrow pK^- K^-$  candidates in fig. 4. Here  $m(pK^-)_{\min}$  indicates the smaller of the two  $m(pK^-)$  values for each signal candidate. The distribution contains a clear peak from the  $\Lambda(1520)$  resonance, a structure that is consistent with being a combination of the  $\Lambda(1670)$  and  $\Lambda(1690)$  states, and possible additional contributions at higher mass. A detailed amplitude analysis will be of interest when larger samples are available.

#### 4. – Conclusions

At LHCb, we now not only observe charmless decays of  $\Lambda_b^0$  baryons but also charmless decays of  $\Xi_b^-$  baryons. Adding Run II data, we will have good prospects to probe the dynamics of charmless  $\Xi_b^-$  decays and to conduct  $CP$ -violation searches. Further in the future, with the LHCb upgrade, detailed studies of these decay modes will become possible.

\* \* \*

The author wishes to thank the organisers of XXXI Rencontres de Physique de la Vallée d'Aoste 2017 for providing the opportunity to present these results. The author also wishes to thank the University of Warwick for supporting this work.

## REFERENCES

- [1] CABIBBO N., *Phys. Rev. Lett.*, **10** (1963) 531.
- [2] KOBAYASHI M. and MASKAWA T., *Prog. Theor. Phys.*, **49** (1973) 652.
- [3] LEES J. P. *et al.*, *Phys. Rev. D*, **13** (2013) 052009.
- [4] DUH Y. T. *et al.*, *Phys. Rev. D*, **87** (2013) 031103.
- [5] AAIJ R. *et al.*, *Phys. Rev. Lett.*, **110** (2013) 221601.
- [6] AAIJ R. *et al.*, *Phys. Rev. Lett.*, **111** (2013) 101801.
- [7] AAIJ R. *et al.*, *Phys. Rev. Lett.*, **112** (2014) 011801.
- [8] AAIJ R. *et al.*, *Phys. Rev. D*, **90** (2014) 112004.
- [9] DALITZ R. *et al.*, *Phys. Rev.*, **94** (1954) 1046.
- [10] AALTONEN T. A. *et al.*, *Phys. Rev. Lett.*, **113** (2014) 242001.
- [11] AAIJ R. *et al.*, *JHEP*, **04** (2014) 087.
- [12] AAIJ R. *et al.*, *Phys. Lett. B*, **759** (2016) 282.
- [13] AAIJ R. *et al.*, *JHEP*, **05** (2016) 081.
- [14] AAIJ R. *et al.*, *Nat. Phys.*, **13** (2017) 391.
- [15] HSIAO Y. K., YAO Y. and GENG C. Q., *Phys. Lett. B*, **95** (2017) 093001.
- [16] AAIJ R. *et al.*, *Phys. Rev. Lett.*, **118** (2017) 071801.
- [17] AAIJ R. *et al.*, *JINST*, **08** (2013) P04022.
- [18] KERZEL U. and FEINDT M., *Nucl. Instrum. Methods A*, **559** (2006) 190.
- [19] PIVK M. and DIBERDER F. R., *Nucl. Instrum. Methods A*, **555** (2005) 356.
- [20] PUNZI G., *Sensitivity of searches for new signals and its optimization*, in *Statistical Problems in Particle Physics, Astrophysics, and Cosmology*, edited by LYONS L., MOUND R. and REITMEYER R. (Imperial College Press) 2003, p. 79.
- [21] ADINOLFI M., *Eur. Phys. J. C*, **73** (2013) 2431.
- [22] ANDERLINI L., LHCb-PUB-2016-021 (2016).
- [23] SKWARNICKI T., DESY-F31-86-02 (1990).
- [24] ALBRECHT H. *et al.*, *Phys. Lett. B*, **241** (1990) 278.